



HAL
open science

MPC2 variants disrupt mitochondrial pyruvate metabolism and cause an early-onset mitochondriopathy

Claire Pujol, Elise Lebigot, Pauline Gaignard, Said Galai, Ichraf Kraoua, Jean-Philippe Bault, Rodolphe Dard, Ilhem Ben Youssef-Turki, Souheil Omar, Audrey Boutron, et al.

► To cite this version:

Claire Pujol, Elise Lebigot, Pauline Gaignard, Said Galai, Ichraf Kraoua, et al.. MPC2 variants disrupt mitochondrial pyruvate metabolism and cause an early-onset mitochondriopathy. *Brain - A Journal of Neurology*, 2022, pp.awac444. 10.1093/brain/awac444. pasteur-03934309

HAL Id: pasteur-03934309

<https://pasteur.hal.science/pasteur-03934309>

Submitted on 11 Jan 2023

HAL is a multi-disciplinary open access archive for the deposit and dissemination of scientific research documents, whether they are published or not. The documents may come from teaching and research institutions in France or abroad, or from public or private research centers.


L'archive ouverte pluridisciplinaire **HAL**, est destinée au dépôt et à la diffusion de documents scientifiques de niveau recherche, publiés ou non, émanant des établissements d'enseignement et de recherche français ou étrangers, des laboratoires publics ou privés.



Distributed under a Creative Commons Attribution - NonCommercial 4.0 International License



MPC2 variants disrupt mitochondrial pyruvate metabolism and cause an early-onset mitochondriopathy

Claire Pujol,^{1,2,†} Elise Lebigot,^{3,†} Pauline Gaignard,³ Said Galai,^{4,5} Ichraf Kraoua,⁵ Jean-Philippe Bault,⁶ Rodolphe Dard,^{6,7} Ilhem Ben Youssef-Turki,⁵ Souheil Omar,⁴ Audrey Boutron,³  Timothy Wai^{1,2,‡} and Abdelhamid Slama^{3,‡}

^{†,‡}These authors contributed equally to this work.

Pyruvate is an essential metabolite produced by glycolysis in the cytosol and must be transported across the inner mitochondrial membrane into the mitochondrial matrix, where it is oxidized to fuel mitochondrial respiration. Pyruvate import is performed by the mitochondrial pyruvate carrier (MPC), a hetero-oligomeric complex composed by interdependent subunits MPC1 and MPC2. Pathogenic variants in the MPC1 gene disrupt mitochondrial pyruvate uptake and oxidation and cause autosomal-recessive early-onset neurological dysfunction in humans. The present work describes the first pathogenic variants in MPC2 associated with human disease in four patients from two unrelated families. In the first family, patients presented with antenatal developmental abnormalities and harboured a homozygous c.148T>C (p.Trp50Arg) variant. In the second family, patients that presented with infantile encephalopathy carried a missense c.2T>G (p.Met1?) variant disrupting the initiation codon. Patient-derived skin fibroblasts exhibit decreased pyruvate-driven oxygen consumption rates with normal activities of the pyruvate dehydrogenase complex and mitochondrial respiratory chain and no defects in mitochondrial content or morphology. Re-expression of wild-type MPC2 restored pyruvate-dependent respiration rates in patient-derived fibroblasts. The discovery of pathogenic variants in MPC2 therefore broadens the clinical and genetic landscape associated with inborn errors in pyruvate metabolism.

- 1 Mitochondrial Biology Group, Institut Pasteur, CNRS UMR 3691, 75015 Paris, France
- 2 Université Paris Cité, 75006 Paris, France
- 3 Biochemistry Department, Bicêtre Hospital, APHP Paris Saclay, 94270 Le Kremlin Bicêtre, France
- 4 Research Laboratory of Neurological Diseases of the Child (LR18SP04), Department of Clinical Biology, Faculty of Medicine of Tunis, National Institute Mongi Ben Hmida of Neurology, University of Tunis El Manar, 1068 Tunis, Tunisia
- 5 Research Laboratory of Neurological Diseases of the Child (LR18SP04), Department of Pediatric Neurology, National Institute Mongi Ben Hmida of Neurology, Faculty of Medicine of Tunis, University of Tunis El Manar, 1068 Tunis, Tunisia
- 6 Department of Gynecology, Poissy—Saint Germain en Laye Hospital, 78300 Poissy, France
- 7 Department of Medical Genetics, Poissy—Saint Germain en Laye Hospital, 78300 Poissy, France

Correspondence to: Timothy Wai
Mitochondrial Biology Group, Institut Pasteur
25 Rue du Docteur Roux, Paris 75015, France
E-mail: timothy.wai@pasteur.fr

Received July 01, 2022. Revised October 19, 2022. Accepted November 12, 2022. Advance access publication November 23, 2022

© The Author(s) 2022. Published by Oxford University Press on behalf of the Guarantors of Brain.

This is an Open Access article distributed under the terms of the Creative Commons Attribution-NonCommercial License (<https://creativecommons.org/licenses/by-nc/4.0/>), which permits non-commercial re-use, distribution, and reproduction in any medium, provided the original work is properly cited. For commercial re-use, please contact journals.permissions@oup.com

Correspondence may also be addressed to: Abdel Slama
Laboratoire de Biochimie, Hôpital de Bicêtre
78 Rue du Général Leclerc, 94270 Le Kremlin-Bicêtre, France
E-mail: abdel.slama-ext@aphp.fr

Keywords: mitochondria; pyruvate carrier; metabolism

Introduction

Pyruvate is a key molecule required for aerobic metabolism. Pyruvate is produced by the cytosolic glycolytic pathway and must be shuttled across the inner mitochondrial membrane (IMM) where it will enter the tricarboxylic acid cycle (TCA cycle or Krebs cycle) to fuel the production of NADH and FADH₂, which serve as electron donors for the respiratory chain.¹ Forty years ago, before the molecular identification of the mitochondrial pyruvate carrier (MPC) complex, the first functional studies suggested a specific and active import of pyruvate into mitochondria.^{2,3} Twenty-five years later, the first patients with impaired mitochondrial pyruvate import were reported.⁴ These patients presented hypotonia, dysmorphia, periventricular cysts, marked metabolic acidosis and hyperlactacidaemia. The lactate/pyruvate (L/P) molar ratios, mitochondrial respiratory chain and pyruvate dehydrogenase (PDH) activities were normal.⁴ It took a decade for the molecular identification of the MPC in eukaryote cells.⁵ The MPC in mammals is composed of two essential and interdependent subunits, MPC1 and MPC2, which must oligomerize in order to form a functional carrier for pyruvate transport across the IMM. Depletion of either subunit provokes the impairment of pyruvate oxidation and pyruvate-driven oxygen consumption.^{5,6} The central role of pyruvate leads to severe and multisystemic metabolic consequences when its transport is impaired.⁷ In rodents, MPC dysfunction contributes to cell proliferation in colorectal or prostate cancer^{8,9} as well as pathological cardiac hypertrophy^{10,11} and diabetic nephropathy,¹² and it has also been shown that MPC is required for myocardial stress adaptation.¹³ In humans, loss-of-function MPC1 variants prevented MPC assembly and mitochondrial pyruvate uptake.^{5,14} To date, there are only 10 patients reported in the literature,¹⁴ with clinical presentations including hypotonia, encephalopathy and frequent early death.^{14,15} Typically, high lactate and pyruvate concentrations with a normal L/P ratio are found in fluids of patients, usually suggesting PDH deficiency. However, MPC impairment should be considered for similar cases. Here, we report the first pathogenic variants in the MPC2 in four patients from two unrelated consanguineous families with pyruvate transport deficiency.

Materials and methods

The full methodology is provided in the [Supplementary material](#).

Data availability

There are no large datasets associated with the study.

Results

Clinical and genetic studies: overview of affected family members

Family 1 is a first-degree consanguineous family (Fig. 1A and Table 1) with two prematurely terminated pregnancies characterized by developmental abnormalities. The first foetus (Patient F1-II.1) was diagnosed prenatally at the second trimester by ultrasound examination with a diffuse subcutaneous oedema,

cardiomegaly, corpus callosum agenesis, ventriculomegaly and a hypoplasia of the cerebellum with hydramnios hyperechogenic punctiform elements in the cerebral parenchyma. The pregnancy was terminated at the 27th week. The second pregnancy resulted in the birth of a healthy daughter (Patient F1-II.2). For the third pregnancy, the foetus (Patient F1-II.3) was examined in the first trimester by ultrasound and presented identical abnormalities to those of the first foetus associated with choroid plexus cysts and domed philtrum, suggesting Fowler's disease (OMIM: 225790; Fig. 1B and C). The pregnancy was subsequently terminated. The karyotype and comparative genomic hybridization array generated from amniotic samples taken from both foetuses (Patients F1-II.1 and F1-II.3) were normal and Fowler's syndrome was ruled out by sequencing of the *FLVCR2* gene.¹⁶ During the third pregnancy, an amniocentesis was performed; PDH activity in the amniotic cell and in the primary cultured fibroblast was in the normal range (Table 1 and Supplementary Table 1).

To pinpoint the genetic origin of the deficit, DNA from the second affected foetus (Patient F1-II.3) was subjected to next-generation sequencing (NGS) using a bespoke panel of 200 nuclear DNA-encoded genes and full mtDNA sequencing, supplemented by a subsequent whole-exome sequencing analysis (Supplementary Table 2). A homozygous variant [c.148T>C, p.(Trp50Arg)] in the MPC2 gene (NM_001143674.4) encoding one of the two subunits of the MPC was identified in this foetus. This variant was absent in ExAC, 1000G or gnomAD databases and modified highly conserved nucleotide and amino acid (Phastcons = 1; conserved amino acid from baker's yeast to human; Fig. 1E). It was predicted to be deleterious according to established algorithms (PolyPhen-2 v.2.2 score: 1.000, MutationTaster score: deleterious). This variant was also confirmed in the first affected foetus by Sanger sequencing in a homozygous state, whereas both parents and their healthy child were heterozygous carriers (Fig. 1A). Thus, the variant could be considered to be a likely pathogenic variant following the American College of Medical Genetics (ACMG) classification (PM1, PM2, PP1, PP3). Our functional studies then allow upgrade of the variant pathogenicity to class 5.

Family 2 is also a first-degree consanguineous family with no family history of a known or suspected genetic condition. The first child (Patient F2-II.1) is a 6-year-old girl. She was initially diagnosed at 8 months of age with an anoxo-ischaemic encephalopathy. This diagnosis was revised at the age of 21 months, when she presented with an isolated dyspnoea associated with elevated levels of lactate in the fasting [4.9 mM, reference values (RV): 0.6–2.2 mM] and postprandial (7.7 mM) states. Brain MRI with spectroscopy and the auditory-evoked potential were normal but the visual-evoked potential was abnormal, pointing to optical pathway impairment. She fed normally without any chewing or swallowing problems but had a severe delayed psychomotor development with no acquisition of sitting position and language. At the age of 5 years, redox cycle in blood showed elevated levels of lactate and pyruvate in the fasting (lactate 5.14 mM and pyruvate 0.239 mM, RV < 0.15 mM) and in postprandial (6.24 and 0.324 mM, respectively) states with normal ratio (15–18 mM, RV < 20 mM). Chromatography of amino acids was normal and chromatography of organic acids showed high lactate level

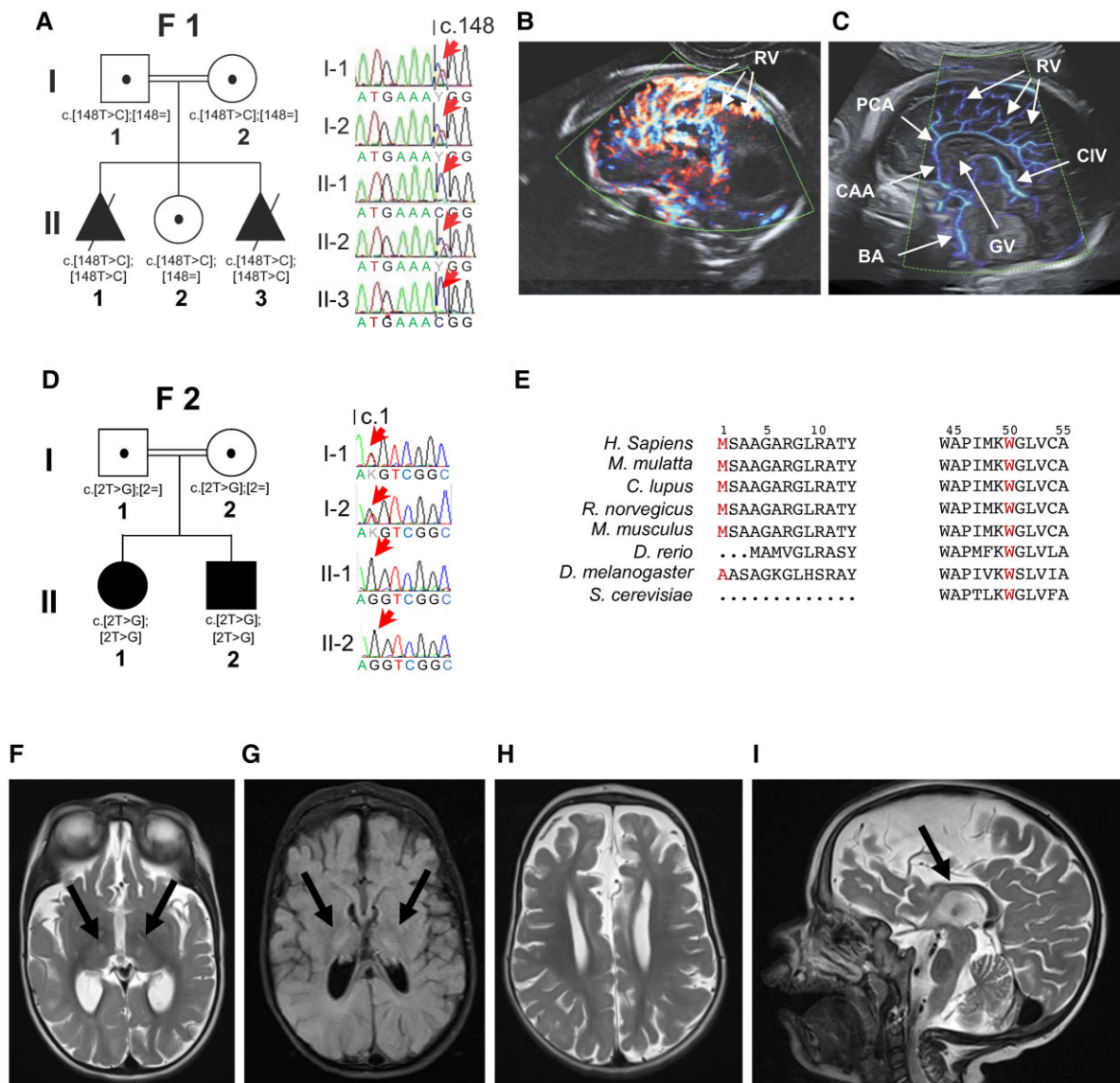


Figure 1 Pedigree and imaging details of MPC2-affected familial individuals carrying deleterious variants. (A) Pedigree of Family 1 (F1) carrying the c.148T>C, p.(Trp50Arg) variant. (B) Cerebral ultrasonographic examination of 24 weeks foetus (Patient F1-II.3) showing important radial vascularization from peri callosal artery (PCA), also seen in Fowler’s disease. (C) Normal brain vascularization in a control foetus at the same term, with basiliary artery (BA); cerebral anterior artery (CAA); peri callosal artery (PCA); radial vascularization (RV); cerebral intern vein (CIV); vein of Galen (GV). (D) Pedigree of Family 2 (F2) carrying the c.2T>G, p.(Met1?) variant. (E) Locations and conservation analysis of the detected variants in MPC2 (in red), conservation of the mutated amino acids is indicated by the alignment of eight species. (F–I) MRI features associated with MPC2 variants in Patient F2-II.2 showing hypoplasia and partial agenesis of the corpus callosum with axial T₂-weighted images (F and H), axial FLAIR (fluid-attenuated inversion recovery) weighted image (G) and sagittal weighted image (I) showing bilateral T₂ and FLAIR hyperintensities of the thalamus as well as cortical, subcortical and corpus callosum atrophy (arrow).

in urine. A PDH deficiency was suspected but excluded after analysis of PDH enzymatic activity and sequencing of the PDHA1 gene, which failed to reveal any defects. The second affected child (Patient F2-II.2) is the younger brother of Patient F2-II.1. His pregnancy was uneventful and his birth was complicated by neonatal respiratory distress, which required 8 days of clinical attention in a neonatal intensive care department. The child presented with phototherapy-responsive neonatal jaundice. At the age of 3 months the parents consulted for hypotonia, excessive head lag and psychomotor retardation. Two months later, the boy acquired the smile response with language at the babbling stage but no motor acquisition was observed. A transfontanellar ultrasound showed dilatation of the third ventricle with

aberrant visualization of the corpus callosum. At 7 months, clinical examination showed poor eye tracking, visual impairment, axial hypotonia with slight segmental hypotonia, weak osteotendinous reflexes in all four limbs, horizontal spontaneous nystagmus, mild coarse facial features with hirsutism and microcephaly (–2 to 3 SD). Brain MRI performed at 2 years showed cortical and subcortical atrophy, hypoplasia of the corpus callosum, T₂ and FLAIR hyperintensity of thalami (Fig. 1F–I). Abdominal and cardiac ultrasounds were normal. Electroneuromyography, visual- and auditory-evoked responses were also normal. Elevated lactate levels in the plasma (8.7 mM) and CSF (10.4 mM, RV: 0.6–2.2 mM) were detected along with high proteinorachia (0.84 g/l, RV < 0.40 g/l). Redox cycle showed

Table 1 Abridged clinical presentation and metabolic findings of patients with homozygous loss-of-function MPC2 variants

	Family 1		Family 2	
	Patient II.1	Patient II.3	Patient II.1	Patient II.2
Year	2012	2017	2016	2019
Sex of the affected individuals	ND	ND	Female	Male
Age at onset	Foetus	Foetus	8 Months	3 Months
Genetic change		c.148T>C ^a		c.2T>G ^a
Allelic genotype		Homozygous		Homozygous
Predicted protein change		p.(Trp50Arg)		p.(Met1?)
Prenatal events	Subcutaneous oedema, cardiomegaly, corpus callosum agenesis, cerebellum hypoplasia, ventriculomegaly		Uneventful	Foetal distress
Phenotype	Post-mortem examination: facial dysmorphism, microcephaly cardiac failure	-	Encephalopathy, dyspnoea, visual impairment	Respiratory distress syndrome, hypotonia, nystagmus, facial dysmorphism, corpus callosum hypoplasia
Developmental delay	MTP 27 wg	MTP 26 wg	Absence of language, inability to reach a seated posture	Severe psychomotor retardation
Blood metabolic findings	-	-	Hyperlactacidaemia (7.32–11.6 mM; NR: 0.79–1.74 mM) Hyperpyruvicaemia (0.48–0.62 mM NR: 0.07–0.13 mM) Normal L/P ratio	Hyperlactacidaemia (5.14–6.24 mM; NR: 0.79–1.74 mM) Hyperpyruvicaemia (0.24–0.32 mM NR: 0.07–0.13 mM) Normal L/P ratio
Tissue metabolic findings	-	Normal PDH activity (amniocyte), decreased pyruvate-stimulated oxygen consumption (fibroblast)	Normal PDH activity	-

MTP = medical termination of pregnancy; ND = not determined; NR = normal range; wg = weeks of gestation.

^aReference transcript of MPC2 is GenBank: NM_001143674.4.

elevated levels of lactate and pyruvate in the fasting (lactate 7.32 mM and pyruvate 0.47 mM) and in postprandial (11.6 and 0.62 mM, respectively) states with normal ratio (15–19; Table 1 and Supplementary Table 1). He is now aged 4 years. He is hypotrophic [weight 10 kg (–3 SD) and height 85 cm (–2 SD)] and has microcephaly [head circumference 45 cm (–3.5 SD)]. His contact and ocular pursuit are poor with irritability and he also has severe generalized hypotonia with no acquisitions and week osteotendinous reflexes.

NGS analysis revealed a previously undescribed homozygous c.2T>G, p.(Met1?) variant in the MPC2 gene in both siblings (Supplementary Table 2). Each parent was found to be a heterozygous carrier of the variant. This variant, absent from public sequencing databases, is predicted to disrupt the initiation codon and was classified as pathogenic according to the ACMG classification criteria (PVS1, PM2 and PP3; Fig. 1D and E).

Molecular studies

To evaluate the impact of the genetic variants identified in MPC2, we analysed the expression of MPC subunits in patient-derived fibroblasts (from Patients F1-II.3 and F2-II.1). Immunoblot analysis revealed severe decreased expression of MPC2 (>90% in both MPC2^{Met1?} and MPC2^{Trp50Arg}) relative to the corresponding control cells obtained from unrelated healthy individuals (Fig. 2A and B). This was accompanied by a marked reduction in the steady-state levels of MPC1 in fibroblasts of both MPC2^{Trp50Arg} and MPC2^{Met1?} patients. These results are in accordance with the literature showing that MPC1 and MPC2 levels are interdependent: the ablation of one

subunit prevents the MPC complex assembly, resulting in the destabilization and subsequent degradation of the other subunit.^{5,6} Indeed, as shown with MPC1^{Arg97Trp}, which is less stable than MPC1^{Lys79His}, the loss of MPC1 leads to MPC2 degradation (Fig. 2A). We did not observe any differences in the steady-state levels of other IMM proteins such as succinate dehydrogenase (SDHB) or ATP5A (Fig. 2A), pointing to a specific defect in the MPC rather than a general decrease in mitochondrial content or IMM proteins. These data were further corroborated by confocal microscopy analysis of mitochondrial content of patient-derived fibroblasts (Supplementary Fig. 1E) labelled with TMRE (tetramethyl rhodamine, ethyl ester), which also did not reveal any obvious alterations in mitochondrial morphology (Supplementary Fig. 1F).

In silico predictions of the MPC2 variants that we identified point to a deleterious loss-of-function effect on MPC2. To prove whether defects in patient-derived fibroblasts are specifically caused by MPC2 dysfunction, we sought to functionally complement them by expressing wild-type MPC2 fused to a haemagglutinin (HA) tag. Stable expression of MPC2-HA at levels comparable to MPC2 levels of control cells was able to rescue MPC1 protein deficiency in MPC2^{Met1?} patient cells (Fig. 2A and B), indicative of a functional rescue of the MPC complex assembly defect.

To determine whether the decreased MPC2 protein levels in patient-derived fibroblasts were the result of reduced stability or synthesis of MPC2 mRNA, we quantified the relative abundance of human MPC1 and MPC2 transcripts by qRT-PCR (Fig. 2C). We detected normal levels of MPC2 transcripts in MPC2^{Met1?} cells in which

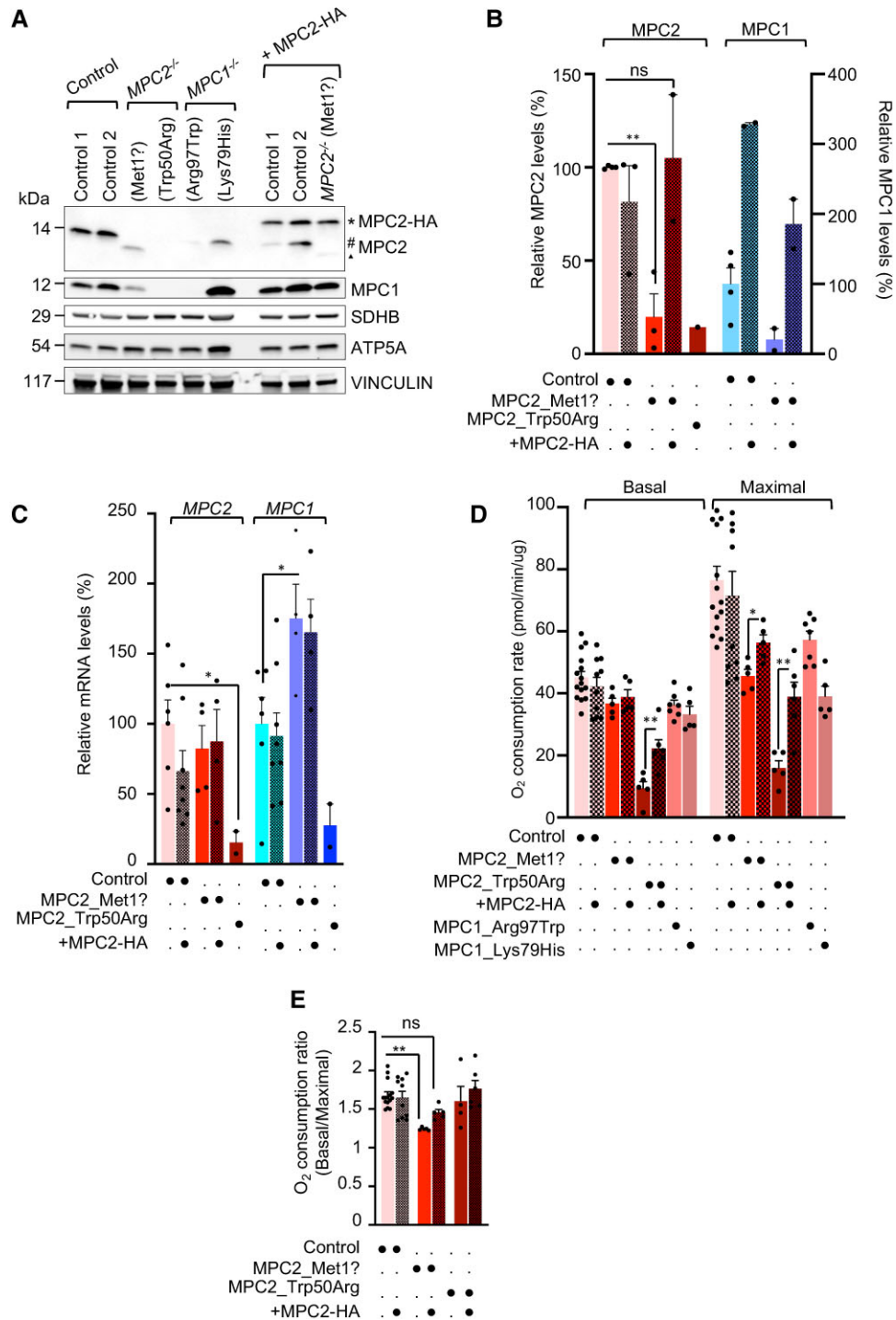


Figure 2 Analysis of MPC1 and MPC2 expression levels. (A) Representative immunoblot of equal amounts of lysates from control (Control 1 and 2), MPC2-deficient fibroblasts before (MPC2^{Trp50Arg} or MPC2^{Met1?}) and after functional complementation with human MPC2-HA (MPC2^{Met1?}+MPC2), and MPC1-deficient (MPC1^{Arg97Trp} or MPC1^{Lys79His}) patient-derived fibroblasts, separated by SDS-PAGE and immunoblotted with the indicated antibodies. An number sign denotes MPC2 native form, triangle denotes truncated MPC2; asterisk denotes MPC2-HA form. (B) Densitometric quantification of MPC2 and MPC1 protein levels in A relative to VINCULIN in patient-derived fibroblasts (n=2–4). (C) Relative MPC2 and MPC1 mRNA levels in patient-derived fibroblasts as compared with controls (n=4). (D and E) Pyruvate-dependent respiration of control (Control 1 and 2), MPC2-deficient fibroblasts (MPC2^{Trp50Arg} or MPC2^{Met1?}) before and after functional complementation with human MPC2-HA (MPC2^{Trp50Arg}+MPC2 or MPC2^{Met1?}+MPC2), and MPC1-deficient (MPC1^{Arg97Trp} or MPC1^{Lys79His}) patient-derived fibroblasts measured by seahorse flux analyser. Basal oxygen consumption was measured in the incubation media without glucose and with pyruvate and maximal respiration was measured after injection of CCCP (carbonyl cyanide m-chlorophenyl hydrazone). All data are presented as mean±SEM and analysed by two-tailed unpaired Student's t-test with (**P≤0.01, *P≤0.05, ns=not significant).

MPC2 protein levels were reduced, suggesting that the MPC2^{Met17} mutation destabilizes MPC2 protein, leading to its proteolytic removal. Interestingly, we observed elevated levels of MPC1 transcript levels in MPC2^{Met17} patient-derived fibroblasts, suggesting a compensatory response to MPC complex dysfunction. For MPC2^{Trp50Arg} patient-derived fibroblasts, we observed markedly reduced levels of both MPC1 and MPC2 transcripts, correlating with reduced protein levels observed by immunoblot analyses. Unfortunately, due to poor growth of MPC2^{Trp50Arg} patient-derived fibroblasts, we were unable to perform in-depth characterization of MPC2^{Trp50Arg} patient-derived fibroblasts. Together, our data indicate that the reduced MPC2 levels observed in MPC2 patient-derived cells is the result of destabilization of mutant MPC2 protein rather than reduced MPC2 transcript levels.

Next, we assessed the pyruvate-dependent respiration of patient-derived fibroblast by measuring basal oxygen consumption in the presence of either pyruvate or glutamate. Glutamate is capable of compensating for mitochondrial pyruvate deficiency by entering the TCA cycle and supports normal respiration rates in MPC1 patient-derived fibroblasts.¹⁵ Yet in the presence of pyruvate (and absence of glutamate), mitochondrial respiration relies exclusively on the redox equivalents generated by intramitochondrial pyruvate pools that require MPC.

Under basal conditions when respiratory substrates are not rate-limiting (Fig. 2D), we did not observe defects in oxygen consumption rates in MPC2 patient-derived fibroblasts. However, upon uncoupler-mediated maximal respiration conditions in which substrates including those of the TCA become rate-limiting, we observed a decrease in pyruvate-dependent oxygen consumption rates in MPC2-deficient fibroblasts (Fig. 2D), as evidenced by the reduced ratio of maximal/basal oxygen consumption rates (Fig. 2E), which could be rescued by restoring MPC2 levels (Fig. 2E). Importantly, we observed no functional defects in glutamate-dependent oxygen consumption rates under basal or uncoupler-mediated maximal respiration conditions (Supplementary Fig. 1G), highlighting a specific defect in pyruvate utilization caused by MPC2 variants identified in these patients. Indeed, cells from individuals with pathogenic variants in MPC1 exhibited impaired pyruvate-dependent respiration defects that could be partially rescued by re-expression of wild-type human MPC1.⁵ Thus, pyruvate-dependent respiration measurements coupled with western blot analysis of MPC subunits represent rapid and effective tools to pinpoint functional defects in the MPC in patient-derived fibroblast.

Discussion

In mitochondria, pyruvate is critical to drive ATP production. Once imported into mitochondria by the MPC, its metabolism is tuned by mainly two enzymes: pyruvate dehydrogenase (PDH), which converts pyruvate to acetyl-coA, and pyruvate carboxylase (PC), which catalyses the conversion of pyruvate to oxaloacetate in fasting conditions. Numerous cases of pathogenic variants disrupting the activity of PDH or PC, and recently MPC1, have been described,^{14,17,18} all leading to severe diseases characterized by various phenotypes including lactic acidosis, hypotonia, developmental delay, seizures and even premature death. Here, we describe the first pathogenic MPC2 variants associated with an equally devastating multisystemic dysfunction in children. Fibroblasts isolated from patients from both families in our study show normal rates of proliferation yet a decreased oxygen consumption rate in the presence of pyruvate but not in the presence of malate and glutamate. Supplementation of fibroblasts from MPC2 patients with the wild-type protein leads to

recovery of pyruvate transport and oxygen consumption (Fig. 2E), even if it remains lower than normal. Together, these data pinpoint the deficiency of the mitochondrial respiratory chain secondary to pyruvate transport impairment.

Our results show that MPC2 deficiency is comparable to that of MPC1 deficiency (Supplementary Table 3). Indeed, both MPC subunits are required to assemble the essential transporter of pyruvate across the IMM. Immunoblot analysis in fibroblasts derived from patients harbouring pathogenic variants in either MPC1 or MPC2 show reduced levels of both subunits of the MPC complex. As observed in *Mpc2* mouse models,¹⁹ we show that hypomorphic MPC2 variants reduce the steady-state levels of MPC2 and thus promote the loss of MPC1, likely through turnover by mitochondrial proteases, which are charged with the task of turnover of mutant and unassembled proteins.²⁰ Inhibiting the turnover of mutant membrane proteins of the IMM has been shown to ameliorate respiratory chain assembly²¹ and confer benefits to preclinical models of neurodegenerative mitochondrial diseases.²² While this paradigm is untested for pyruvate transport deficiencies, future studies should identify the mitochondrial proteases responsible for the turnover of mutant MPC subunits and determine whether impairing this degradation may lead to amelioration in the assembly and activity of the MPC complex.

Acknowledgements

We thank the patients and their families. We thank Elodie Vimont for technical assistance, Izabela Sumara from the IGBMC for the HeLa FlpN TRex cells, Sylvie Fabrega of the Viral Vector for Gene Transfer core facility of Structure Fédérative de Recherche Necker, Université Paris Cité for lentiviral particle synthesis and Marie Lemesle for excellent administrative assistance.

Funding

T.W. is supported by the European Research Council (ERC) Starting Grant No. 714472 (Acronym 'Mitomorphosis'). T.W. and C.P. are supported by the French National Center for Scientific Research (CNRS). E.L., P.G. and A.S. are supported by the AMMI 'Association contre les Maladies Mitochondriales'. S.G. is supported by Tunisian Ministry of High Education and Scientific Research through the Junior Project 'Jeune Enseignant Chercheur PJEC'.

Competing interests

The authors declare no competing interests.

Supplementary material

Supplementary material is available at *Brain* online.

References

1. Fink JK. Hereditary spastic paraplegia: Clinico-pathologic features and emerging molecular mechanisms. *Acta Neuropathol.* 2013;126:307-328.
2. Halestrap AP. Stimulation of pyruvate transport in metabolizing mitochondria through changes in the transmembrane pH gradient induced by glucagon treatment of rats. *Biochem J.* 1978; 172:389-398.

3. Papa S, Paradies G. On the mechanism of translocation of pyruvate and other monocarboxylic acids in rat-liver mitochondria. *Eur J Biochem.* 1974;49:265-274.
4. Brivet M. Impaired mitochondrial pyruvate importation in a patient and a fetus at risk. *Mol Genet Metab.* 2003;78:186-192.
5. Bricker DK, Taylor EB, Schell JC, et al. A mitochondrial pyruvate carrier required for pyruvate uptake in yeast, drosophila, and humans. *Science.* 2012;337:96-100.
6. Herzig S, Raemy E, Montessuit S, et al. Identification and functional expression of the mitochondrial pyruvate carrier. *Science.* 2012;337:93-96.
7. Zangari J, Petrelli F, Maillot B, Martinou JC. The multifaceted pyruvate metabolism: Role of the mitochondrial pyruvate carrier. *Biomolecules.* 2020;10:1068.
8. Schell JC, Olson KA, Jiang L, et al. A role for the mitochondrial pyruvate carrier as a repressor of the Warburg effect and colon cancer cell growth. *Mol Cell.* 2014;56:400-413.
9. Kuerbanjiang M, Gu L, Xu C, et al. Decreased expression of MPC2 contributes to aerobic glycolysis and colorectal cancer proliferation by activating mTOR pathway. *J Immunol Res.* 2021;2021:1-12.
10. Fernandez-Caggiano M, Kamynina A, Francois AA, et al. Mitochondrial pyruvate carrier abundance mediates pathological cardiac hypertrophy. *Nat Metab.* 2020;2:1223-1231.
11. Fernandez-Caggiano M, Eaton P. Heart failure—Emerging roles for the mitochondrial pyruvate carrier. *Cell Death Differ.* 2021;28:1149-1158.
12. Zhu H, Wan H, Wu L, et al. Mitochondrial pyruvate carrier: A potential target for diabetic nephropathy. *BMC Nephrol.* 2020;21:274.
13. Zhang Y, Taufalele PV, Cochran JD, et al. Mitochondrial pyruvate carriers are required for myocardial stress adaptation. *Nat Metab.* 2020;2:1248-1264.
14. Jiang H, Alahmad A, Fu S, et al. Identification and characterization of novel MPC1 gene variants causing mitochondrial pyruvate carrier deficiency. *J Inher Metab Dis.* 2022;45:264-277.
15. Oonthonpan L, Rauckhorst AJ, Gray LR, Boutron AC, Taylor EB. Two human patient mitochondrial pyruvate carrier mutations reveal distinct molecular mechanisms of dysfunction. *JCI Insight.* 2019;4:e126132.
16. Meyer E, Ricketts C, Morgan NV, et al. Mutations in *FLVCR2* are associated with proliferative vasculopathy and hydranencephaly-hydrocephaly syndrome (Fowler syndrome). *Am J Hum Genet.* 2010;86:471-478.
17. Ganetzky R, McCormick EM, Falk MJ, et al. Primary pyruvate dehydrogenase complex deficiency overview. In: Adam MP, Ardinger HH and Pagon RA, editors. *GeneReviews*®. University of Washington; 1993.
18. Wang D, De Vivo D, et al. Pyruvate carboxylase deficiency. In: Adam MP, Ardinger HH and Pagon RA, editors. *GeneReviews*®. University of Washington; 1993.
19. Vigueira PA, McCommis KS, Schweitzer GG, et al. Mitochondrial pyruvate carrier 2 hypomorphism in mice leads to defects in glucose-stimulated insulin secretion. *Cell Rep.* 2014;7:2042-2053.
20. Ng MYW, Wai T, Simonsen A. Quality control of the mitochondrion. *Dev Cell.* 2021;56:881-905.
21. Hornig-Do HT, Tatsuta T, Buckermann A, et al. Nonsense mutations in the COX1 subunit impair the stability of respiratory chain complexes rather than their assembly: Turnover of mitochondrial proteins. *EMBO J.* 2012;31:1293-1307.
22. Rummyantseva A, Popovic M, Trifunovic A. CLPP deficiency ameliorates neurodegeneration caused by impaired mitochondrial protein synthesis. *Brain.* 2022;145:92-104.